Supplementary Information for

"The free energy cost of accurate biochemical oscillations" by Cao et al.

I. DESCRIPTIONS OF THE FOUR MODELS

Here, we describe the mathematical details of the four models of biochemical oscillations studied in this paper. For the activator-inhibitor and the glycolysis model, we only give the ordinary differential equations (ODE's) to describe the deterministic part of the chemical reactions. The actual simulations of the stochastic reactions were done using Gillespie algorithm (see Methods in the main text). For the repressilator and brusselator models, we use the chemical master equation (or Langevin equation with Poisson noise) and solve the corresponding Fokker-Planck equation:

$$\frac{\partial P(\vec{x},t)}{\partial t} = -\nabla(\mathbf{F}P - \mathbf{D}\nabla P) = -\nabla J, \tag{S1}$$

where $\mathbf{F}$ is the force vector, and $\mathbf{D}$ is the noise matrix. J is the flux vector for each direction.

In all our models, the units of the parameters are composed of concentration (c, arbitrary), time (t, arbitrary) and volume (V, arbitrary). The molecule number unit $c \times V$ represents the real counts of a given molecule in the system. For example, if the concentration of enzyme E is $E_T = 10(c)$, and the volume is $V = 100(V)$, then the total number of enzyme E in our system is $E_T V = 1000$. The dependence of the amplitude and the period of the oscillations versus energy dissipation for all the four models studied in this paper are shown in Fig. S1.

A. Activator-inhibitor model

The main components of the model are the activator R and its inhibitor X. R and X are linked in a feedback loop through a phosphorylation-dephosphorylation (PdP) cycle (main text Fig. 1b). R activates the synthesis of both R and X through phosphorylated enzyme M, thus forms a positive feedback; at the same time, X degrades R, thus forms a negative feedback. The parameter $\gamma = d_1 d_2 f_{-1} f_{-2}/(a_1 a_2 f_1 f_2)$ is introduced to distinguish wether the

system is in equilibrium ($\gamma = 1$) or non-equilibrium ($0 < \gamma < 1$). The kinetics is described by:

$$\begin{aligned}
\frac{d[R]}{dt} &= k_0[M_p] + k_1 S - k_2[X][R] \\
\frac{d[X]}{dt} &= k_3[M_p] - k_4[X] \\
\frac{d[M]}{dt} &= f_2[M_pK] + d_1[MR] - a_1[M]([R] - [MR]) - f_{-2}[M][K] \\
\frac{d[MR]}{dt} &= a_1[M]([R] - [MR]) + f_{-1}[M_p]([R] - [MR]) - (f_1 + d_1)[MR] \\
\frac{d[M_p]}{dt} &= f_1[MR] + d_2[M_pK] - a_2[M_p][K] - f_{-1}[M_p]([R] - [MR]) \\
\frac{d[M_pK]}{dt} &= a_2[M_p][K] + f_{-2}[M][K] - f_2[M_pK] - d_2[M_pK]
\end{aligned} \tag{S2}$$

with two mass conservation constraints: $[M] + [M_p] + [MR] + [M_pK] = M_T, [M_pK] + [K] = K_T$, where M_T and K_T are the total concentrations of enzyme M and phosphatase K. Each term in the equations represents one of the reactions in the main text (see Fig. 1b). We take symmetric parameters: $k_0 = k_1 = k_3 = 1(t^{-1}), k_2 = 1(c^{-1}t^{-1}), k_4 = 0.5(t^{-1}), S = 0.4(c), K_T = 1(c), M_T = 10(c), a_1 = a_2 = 100(c^{-1}t^{-1}), f_1 = f_2 = d_1 = d_2 = 15(t^{-1}), f_{-1} = f_{-2} = \sqrt{\gamma} a_1 f_1/d_1(c^{-1}t^{-1})$. The oscillation onset point is at $\gamma_c = 2 \times 10^{-3}$. Notice that the PdP cycle's reaction rates are much larger than the reactions of synthesis and degradation of R and X, so the total R is almost unchanged in the time scale of the PdP cycles.

B. Repressilator

We use the simplified cell cycle model in[1], where CDK activates Plk1, and Plk1 activates APC, which inhibits CDK in return. The (deterministic) negative feedback loop kinetics are governed by the following ODE's, with CDK, Plk1, APC concentrations represented by x, y, z, respectively:

$$\begin{aligned}
\frac{dx}{dt} &= \alpha_1 - \beta_1 \frac{z^{n_1}}{K_1^{n_1} + z^{n_1}} = f_x - d_x \\
\frac{dy}{dt} &= \alpha_2 (1 - y) \frac{x^{n_2}}{K_2^{n_2} + x^{n_2}} - \beta_2 y = f_y - d_y \\
\frac{dz}{dt} &= \alpha_3 (1 - z) \frac{y^{n_3}}{K_3^{n_3} + y^{n_3}} - \beta_3 z = f_z - d_z
\end{aligned} \tag{S3}$$

where f_i, d_i are the synthesis and decay rates of each component. We chose $\alpha_1 = 0.1(ct^{-1}), \alpha_2 = 3(t^{-1}), \beta_1 = 3(ct^{-1}), \beta_2 = 1(t^{-1}), \beta_3 = 1(t^{-1}), K_1 = 0.5(c), K_2 = 0.5(c), K_3 = 0.5(c), n_1 =$

$8, n_2 = 8, n_3 = 8$, and $\alpha_3(t^{-1})$ is taken as the control parameter ranges from 1.0 to 3.0. The oscillation onset point is $\alpha_3 = 0.8$.

The full stochastic dynamics is described by the Fokker-Planck equation (Eq. S1) with the force vector and noise matrix given by:

$$\mathbf{F} = [f_x - d_x, f_y - d_y, f_z - d_z], \quad \mathbf{D} = \frac{1}{2V} diag[f_x + d_x, f_y + d_y, f_z + d_z]$$

.

C. Brusselator

The brusselator is composed of three reactions, $A \to X$, $B \to Y$, and $2X + Y \to 3X$. X will degrade in a constant rate. The deterministic equation of brusselator is

$$\begin{aligned} \frac{dx}{dt} &= a - x + x^2 y, \\ \frac{dy}{dt} &= b - x^2 y. \end{aligned} \tag{S4}$$

where x, y are the normalized concentration of X, Y.

The Fokker-Planck equation was derived from chemical master equations (CME) in [2], which gave:

$$\mathbf{F} = \begin{pmatrix} a - x + x^2 y \\ b - x^2 y \end{pmatrix} + \frac{1}{2V} \begin{pmatrix} -1/2 - 2xy + x^2/2 \\ 2xy - x^2/2 \end{pmatrix} \tag{S5a}$$

$$\mathbf{D} = \frac{1}{2V} \begin{pmatrix} a + x + x^2 y & -x^2 y \\ -x^2 y & b + x^2 y \end{pmatrix} \tag{S5b}$$

where V is the volume of the system. We used $b = 0.4$, and varied $a \in [0.12, 0.18]$ in our study. Fig. S2 gives two examples of probability distribution $P(\vec{x}, t)$ and fluxes J in the brusselator model.

D. Glycolysis oscillation

The glycolysis model in our study is taken from [3], but we have introduced finite reverse reaction rates for the catalysis processes to study the free energy dissipation in glycolysis. The enzyme PFK are composed of n protomers, and undergoes allosteric regulation by its product P. Each protomer exists two states, R, which has catalytic activity for converting

substrate S to P, and T, which is inactive. Assuming a quasi-equilibrium of the allosteric states of PFK [3], the dynamics of S and P can be written as:

$$\begin{aligned}\frac{dS}{dt} &= v_i - \frac{nD(1+\alpha)^{n-1}(1+\theta)^n(k\alpha - k'P)}{L+(1+\alpha)^n(1+\theta)^n} \\ \frac{dP}{dt} &= \frac{nD(1+\alpha)^{n-1}(1+\theta)^n(k\alpha - k'P)}{L+(1+\alpha)^n(1+\theta)^n} - k_s P\end{aligned} \tag{S6}$$

where $\alpha = (a_1 S + k'P)/(k+d_1), \theta = a_2 P/d_2$. Parameters were chosen as $D = 500(c), n = 2, a_1 = a_2 = 10(c^{-1}t^{-1}), d_1 = d_2 = 10(t^{-1}), k = 1(t^{-1}), v_i = 0.2(ct^{-1}), k_s = 0.1(t^{-1}), L = 7.5 \times 10^6$. $k'(c^{-1}t^{-1})$ is the reverse reaction rate of P to S. The oscillation onset point is $k' = 4 \times 10^{-1}$. Stochastic simulations were performed for 4 reactions: synthesis of S, degradation of P, catalysis of S to P, reverse reaction of P to S. Here, we combined all the enzymatic reactions into two reactions since the transitions between different allosteric states of the enzyme are much faster than the slow reactions of substrate injection (v_i) and product removal (k_s).

The dissipation of the system can be directly calculated by summing up the dissipation of all the enzymatic reactions:

$$\Delta W(t) = \frac{nD(1+\alpha)^{n-1}(1+\theta)^n(k\alpha - k'P)}{L+(1+\alpha)^n(1+\theta)^n} \times \log\frac{ka_1 S}{k'd_1 P} = N_S \times \Delta G, \tag{S7}$$

where N_S quantifies how many molecules of S are catalysed to P.

II. ENERGY DISSIPATION DETERMINED FROM SOLVING THE FOKKER-PLANCK EQUATION

Consider a general Fokker-Planck equation

$$\frac{\partial P(\vec{x},t)}{\partial t} = -\nabla(\mathbf{F}P - \mathbf{D}\nabla P) = -\nabla J \tag{S8}$$

where $\mathbf{F}$ is the force vector, and $\mathbf{D}$ is the noise matrix. J is the flux vector for each direction. The system's entropy is

$$S(t) = -\int P(\vec{x},t)\ln P(\vec{x},t)d\vec{x} \tag{S9}$$

The entropy production rate is[4]:

$$\frac{dS(t)}{dt} = -\int [\ln P(\vec{x},t)+1]\frac{\partial P(\vec{x},t)}{\partial t}d\vec{x} = \int [\ln P(\vec{x},t)+1]\nabla J d\vec{x} \tag{S10}$$

Integrated by parts:

$$\frac{dS(t)}{dt} = -\int J^T \nabla \ln P(\vec{x},t) d\vec{x} \tag{S11}$$

where J^T is the transposition of J. By definition $J = \mathbf{F}P - \mathbf{D}\nabla P$, we have

$$J^T \nabla \ln P = J^T \mathbf{D}^{-1}\mathbf{F} - \frac{J^T \mathbf{D}^{-1} J}{P} \tag{S12}$$

Finally

$$\frac{dS(t)}{dt} = -\int J^T \mathbf{D}^{-1}\mathbf{F} d\vec{x} + \int \frac{J^T \mathbf{D}^{-1} J}{P} d\vec{x} \tag{S13}$$

The second term is the free energy dissipation rate (also called entropy production rate[5]) in unit of $k_B T_r$, where T_r is the room temperature or the temperature where the reactions occur.

III. ONSET OF OSCILLATION

Systems at the onset of oscillation is dissipative. In Fig. S1, we show that at the onset of oscillation, i.e., when amplitude is zero, the free energy dissipation is finite positive.

IV. SIMULATION RESULTS OF REPRESSILATOR, BRUSSELATOR AND GLYCOLYSIS MODEL

We perform the same simulation as the activator-inhibitor model for repressilator, brusselator and glycolysis. The relation between energy dissipation and phase diffusion are shown in Fig. S3, with the scaling analysis in each of the insets. The data can be fitted well with equation $V \times D/T = C + W_0/(\Delta W - W_c)$, with the fitting parameters given in the caption. These result show the generality of the inverse relation between energy dissipation and phase diffusion.

V. EFFICIENCY AND MATCH OF PARAMETERS

To optimize efficiency is equivalent to finding the minimum phase fluctuation with a constant energy dissipation. We set up a simple scheme to gain an intuitive understanding of the choices of parameters for optimizing efficiency. We consider a biased random walker on a discrete ring with N sites $i = 1, 2...N$. Different site can be considered as different phase

in the oscillation cycle. At site i the forward rate is f_i, and reverse rate is $f_i\gamma_i$ ($\gamma_i \ll 1$). The average time from arriving at site i to leaving for site $i+1$ is $t_i = 1/(f_i - f_i\gamma_i)$, with variance (site/phase uncertainty) of $(f_i + f_i\gamma_i)t_i$. Therefore, starting from site 1, when arriving site N (a full cycle), the accumulated variance will be:

$$\Sigma_T = \sum_{i=1}^{N}(f_i + f_i\gamma_i)t_i = \sum_{i=1}^{N}\frac{1+\gamma_i}{1-\gamma_i} \approx \sum_{i=1}^{N} 1 + 2\gamma_i. \tag{S14}$$

A constant energy dissipation (per cycle) requires that $\prod_{i=1}^{N}\gamma_i = \gamma$ is a constant. It is easy to see that Σ_T will approach its minimum when $\gamma_i = \sqrt[N]{\gamma}$ is the same for all steps in the ring.

In the activator-inhibitor model, $\gamma_1 = d_1[MR]/(a_1[M][R])$, $\gamma_2 = f_{-1}[M_p][R]/(f_1[MR])$, $\gamma_3 = d_2[M_pK]/(a_2[M_p][K])$, $\gamma_4 = f_{-2}[M][K]/f_2[M_pK]$. Constrain on energy is $\gamma_1\gamma_2\gamma_3\gamma_4 = const.$ According to the discussions above, the minimum phase fluctuation is achieved when $\gamma_1 = \gamma_2 = \gamma_3 = \gamma_4$. For the choices of parameters we used in this study, we have on average (over time) $[R] \approx [K], [M] \approx [M_p]$, and $[MR] \approx [M_pK]$, thus the optimum efficiency conditions correspond to $a_1 \approx a_2$ and $f_{-1} \approx f_{-2}$. Based on the relation between a_1, f_{-1}, f_{-2} and $[ATP], [ADP], [P_i]$, the conditions of $a_1 = a_2$ and $f_{-1} = f_{-2}$ lead to $[ATP] = 10^3, [ADP] = [P_i]$.

VI. EXPERIMENTAL DATA ANALYSIS

The experimental data were obtained from Ref[6] and Ref[7]. The data were processed to calculate the autocorrelation function and fitted the autocorrelation function with exponentially decay function $A\cos(2\pi t/T)e^{-t/\tau}$, from which the period T and correlation time τ could be obtained. See Fig. S4.

VII. AMPLITUDE FLUCTUATION, PHASE DIFFUSION AND ENERGY DISSIPATION IN THE STUART-LANDAU EQUATION

The noisy Stuart-Landau equation for x, y:

$$\begin{aligned}\frac{dx}{dt} &= (ax - by) - (cx + dy)(x^2 + y^2) + \eta_1(t) = F_x + \eta_1(t),\\ \frac{dy}{dt} &= (bx + ay) - (cy - dx)(x^2 + y^2) + \eta_2(t) = F_y + \eta_2(t),\end{aligned} \tag{S15}$$

where $a,\ b,\ c,\ d,\ (b, c, d > 0)$ are real variables, and $\langle \eta_i(t)\eta_j(t')\rangle = 2\Delta\delta_{ij}\delta(t-t')$. The corresponding equation in polar coordinates are:

$$\frac{dr}{dt} = ar - cr^3 + \eta_r, \quad \frac{d\theta}{dt} = b + dr^2 + \eta_\theta. \tag{S16}$$

where $\eta_r = \eta_1(t)\cos\theta + \eta_2(t)\sin\theta$, and $\eta_\theta = -\eta_1(t)\sin\theta/r + \eta_2(t)\cos\theta/r$. For $a > 0$, the system starts to oscillate with a mean amplitude $r_s = \sqrt{\frac{a}{c}}$.

We first derive the amplitude fluctuation. The deviation in r can be defined as

$$\delta r = r - r_s, \tag{S17}$$

where $r_s = \sqrt{a/c}$. Perturbation δr near r_s follows the equation (in first order approximation):

$$\frac{d(\delta r)}{dt} = -2a\delta r + \eta_r(t). \tag{S18}$$

Following [8], as $t \to \infty$, we obtain the amplitude fluctuation:

$$\langle \delta r^2(\infty)\rangle = \frac{\Delta}{2a}, \tag{S19}$$

Phase can be defined without ambiguity when $r_s > \sqrt{\Delta/2a}$. This leads to $a > \sqrt{2c\Delta}$. When Δ is small, the phase diffusion constant is determined by expanding the phase velocity around $r = r_s$. This leads to $d\theta/dt = b + dr_s^2 + \beta\delta r(t) + \eta_\theta(t)$, with $\beta \equiv \partial\omega(r_s)/\partial r = 2d\sqrt{a/c}$. Approximately, we have $\langle\dot{\theta}\rangle = 0$, $\langle\eta_\theta(t)\eta_\theta(t')\rangle \approx \Delta/r^2\delta(t-t') \approx \Delta/r_s^2\delta(t-t')$. The phase fluctuation $\delta\theta \equiv \theta - \omega(r_s)t$ follows diffusion with the diffusion constant given by:

$$\begin{aligned}\langle\theta^2\rangle - \langle\theta\rangle^2 &= \int_0^t\int_0^t (\langle\omega(\tau_1)\omega(\tau_2)\rangle - \langle\omega(\tau_1)\rangle\langle\omega(\tau_2)\rangle)d\tau_1 d\tau_2 \\ &= \beta^2\int_0^t\int_0^t [\langle\delta r(\tau_1)\delta r(\tau_2)\rangle - \langle\delta r(\tau_1)\rangle\langle\delta r(\tau_2)\rangle]d\tau_1 d\tau_2 + \Delta t/r_s^2.\end{aligned} \tag{S20}$$

Following [8], as $t \to \infty$, we have:

$$\langle\theta^2\rangle - \langle\theta\rangle^2 = (\beta^2\frac{\Delta}{2a^2} + \frac{\Delta}{r_s^2})t \equiv D_\theta t. \tag{S21}$$

The Fokker-Planck equation for Eq. S15 is:

$$\frac{\partial P}{\partial t} = -\frac{\partial}{\partial x}(F_x P - \Delta\frac{\partial P}{\partial x}) - \frac{\partial}{\partial y}(F_y P - \Delta\frac{\partial P}{\partial y}) = -\frac{\partial J_x}{\partial x} - \frac{\partial J_y}{\partial y}. \tag{S22}$$

where J_x and J_y are the probability density fluxes in phase space. It's more convenient to write Eq. S22 in polar coordinates:

$$\frac{\partial P}{\partial t} = -\frac{1}{r}\frac{\partial}{\partial r}[(ar - cr^3)rP - r\Delta\frac{\partial P}{\partial r}] - \frac{\partial}{\partial\theta}[(b + dr^2)P - \frac{\Delta}{r^2}\frac{\partial^2 P}{\partial\theta^2}]. \tag{S23}$$

Since $\omega(r) = b + dr^2$ does not depend on θ, the steady state probability distribution $P_s(r,\theta)$ only depends on r:

$$P_s(r,\theta) = P(r) = A\exp\left[-\frac{(cr^4/4 - ar^2/2)}{\Delta}\right], \tag{S24}$$

where $A = \left[2\pi\int \exp\left[-(cr^4/4 - ar^2/2)/\Delta\right] r dr\right]^{-1}$ is the normalization constant.

Following Section II.E of the main text, we obtain the minimum free energy dissipation:

$$\dot{W} = k_B T_e \int\int [\frac{J_x^2}{\Delta P} + \frac{J_y^2}{\Delta P}] dxdy = k_B T_e \int\int \frac{r^2\omega^2 P}{\Delta} r dr d\theta. \tag{S25}$$

where T_e is an (effective) temperature of the environment, we set $k_B T_e = 1$ here. The period of the oscillation is $T = 2\pi/\langle\omega(r)\rangle$. The energy dissipated in one cycle is:

$$\Delta W = \dot{W}T = \frac{2\pi\langle r^2\omega^2\rangle}{\Delta\langle\omega\rangle}. \tag{S26}$$

The explicit expression for energy dissipation is:

$$\Delta W = 2\pi\frac{\sqrt{c\Delta}(2a^2d^2 + 8d^2c\Delta + 4abcd + 2b^2c^2) + e^{a^2/4c\Delta}\sqrt{\pi}f(a)[a(bc+ad)^2 + 2cd(2bc+3ad)\Delta]}{c^2\Delta[2d\sqrt{c\Delta} + (bc+ad)e^{a^2/4c\Delta}\sqrt{\pi}f(a)]}, \tag{S27}$$

where $f(a) = 1 + erf(a/2\sqrt{c\Delta})$, with erf the error function. When $a > 2\sqrt{c\Delta}$ and Δ is small, the term $e^{a^2/4c\Delta}$ dominates, which gives:

$$\begin{aligned}\Delta W &\approx 2\pi\frac{a(bc+ad)^2 + 2cd(2bc+3ad)\Delta}{c^2\Delta(bc+ad)} \\ &= \frac{2\pi da^2}{c^2\Delta} + \frac{2\pi ba}{c\Delta} + \frac{4\pi d^2 a}{c(ad+bc)} + \frac{8\pi d}{c}.\end{aligned} \tag{S28}$$

ΔW depends linearly on a in the region of $a << bc/d$, which gives the upper bound of the inverse relation between energy dissipation and phase diffusion. When $d \to 0$, the upper bound goes to infinity, and $W_c \to 0$.

Beyond the upper bound ($a > \frac{bc}{d}$), the energy dissipation will be dominated by higher order terms in a, e.g., a^2 term. The inverse relation will be corrected by terms like $(\Delta W - W_c)^{-1/2}$, which decreases slower than $(\Delta W - W_c)^{-1}$. The nonlinear term of a^2 in dissipation is caused by the phase-amplitude correlation parameter d. When $d = 0$ (which means the phase direction is independent of amplitude), the upper bound will vanish. This implies the inverse relation between energy dissipation and phase diffusion are valid in a relatively large region when the phase-amplitude coupling is not strong.

In Fig. S5, we give the simulation results for $b = 1, d = 1, c = 1, \Delta = 0.02$. The inverse relation between energy dissipation and phase diffusion is valid in a finite region (region

II shown in Fig. S5 b). In this region, the simulation result agrees well with the inverse relation predicted in Eq. 12 in the main text.

A. C is finite when $\Delta_1 \neq \Delta_2$.

Here we show that in the generic case where Δ_1 and Δ_2 vary independently, C, the phase diffusion at the infinite dissipation limit $\Delta W \to \infty$, is finite. We first show this analytically in the limit when Δ_1 and Δ_2 are both small. In this limit, $\langle \eta_r(t)\eta_r(t')\rangle = \delta(t-t')(\Delta_1\langle\cos^2\theta\rangle + \Delta_2\langle\sin^2\theta\rangle)$, and $\langle\eta_\theta(t)\eta_\theta(t')\rangle \approx (\Delta_1\langle\cos^2\theta\rangle + \Delta_2\langle\sin^2\theta\rangle)/r_s^2$. Averaging in sufficient long period, i.e., $t = nT,\ n \to \infty$, gives $\int_0^t\langle\cos^2\theta\rangle dt = \int_0^t\langle\sin^2\theta\rangle dt = 1/2$. The phase diffusion constant will be:

$$D_\theta = \frac{\Delta_1+\Delta_2}{2a}(\frac{d^2}{2c}+c) = \frac{\kappa}{2a}\Delta_1 + \frac{\kappa}{2a}\Delta_2. \tag{S29}$$

The energy dissipation in one cycle is:

$$\Delta W = \frac{2\pi}{\omega(r_s)}\int\int[\frac{J_x^2}{\Delta_1 P}+\frac{J_y^2}{\Delta_2 P}]dxdy \approx \frac{2\pi}{\omega(r_s)}[\frac{\int\int F_x^2 P dxdy}{\Delta_1}+\frac{\int\int F_y^2 P dxdy}{\Delta_2}] \approx \frac{W_1}{\Delta_1}+\frac{W_2}{\Delta_2}. \tag{S30}$$

When $\Delta_1, \Delta_2 \to 0$, $P_r(r) \to \delta(r-r_s)$ and $W_1 = W_2$ are finite constants determined by a, b, c, d. In a realistic system, noise can come through different degrees of freedom, some of which are controlled and some are not. Here, we use Eq. S29 and Eq. S30 to study this general situation. By keeping Δ_1 as a small constant and varying Δ_2 continuously, the inverse relationship between phase diffusion and energy dissipation can be obtained by eliminating Δ_2:

$$D_\theta = C + \frac{W_0}{\Delta W - W_c}, \tag{S31}$$

where $C = \kappa\Delta_1/2a$, $W_c = W_1/\Delta_1$, and $W_0 = \kappa W_2/2a$ are *finite* constants dependent on model parameters (a, b, c, d, and Δ_1).

In Fig. S6, we show the simulation results of a specific case with fixed $\Delta_1 = 0.1$ while varying $\Delta_2 \in [0.05, 0.2]$. We found that the onset, which corresponds to $D \to \infty$, occurs at a finite energy dissipation $W_c \neq 0$ (Fig. S6a). As $\Delta_2 \to 0$, which corresponds to $\Delta W \to \infty$, D approaches a non-zero constant $C \approx 0.0011$ as there is still non-zero fluctuation in the x direction that is not suppressed by free energy dissipation. Overall, the general relationship of $D/T = W_0/(\Delta W - W_c) + C$, with $C \neq 0$, holds true with finite values of W_0, W_c, and C

as shown in Fig. S6b. Note that in the main text, we considered the symmetric case with $\Delta_1 = \Delta_2$. Taking the limit $\Delta_1 = \Delta_2 \to 0$ in Eq. S29 and Eq. S30, it is easy to see that $D_\theta \to 0$ and $\Delta W \to \infty$, therefore $C = 0$ in the symmetric model.

VIII. AMPLITUDE FLUCTUATION

The (minimum) amplitude fluctuation can be defined as the dispersion of the stochastic trajectories departing from the deterministic trajectory in phase-space:

$$d^2 = \int \min\left(\vec{x} - \vec{x}_d\right)^2 P(\vec{x}) d\vec{x} \tag{S32}$$

where $\vec{x}_d$ are the points on the deterministic trajectory. In the four models we studied, the amplitude fluctuations decrease with energy dissipation and scale with $1/\sqrt{V}$, as shown in Fig. S7.

IX. ROBUSTNESS AND ENERGY DISSIPATION

For the activator-inhibitor model, the total number of enzyme E and phosphatase K may vary in real systems (e.g., from cell to cell). Here we search the parameter space of (M_T, K_T) in the region $M_T \in [0, 1000]$ and $K_T \in [0, 2]$, and check wether the system oscillates (with amplitude larger than 0.1) for different values of γ. Robustness is defined as the area in the parameter space where oscillation exists. We found robustness increases as the system becomes more irreversible or equivalently dissipates more free energy, as shown in Fig. S8.

---

[1] Ferrell, J. J., Tsai, T. Y. & Yang, Q. Modeling the cell cycle: why do certain circuits oscillate? *Cell* **144**, 874–85 (2011).

[2] Qian, H., Saffarian, S. & Elson, E. L. Concentration fluctuations in a mesoscopic oscillating chemical reaction system. *Proc Natl Acad Sci U S A* **99**, 10376–81 (2002).

[3] Goldbeter, A. & Lefever, R. Dissipative structures for an allosteric model. application to glycolytic oscillations. *Biophys J* **12**, 1302–15 (1972).

[4] Tome, T. & de Oliveira, M. J. Entropy production in irreversible systems described by a fokker-planck equation. *Phys Rev E* **82**, 021120 (2010).

[5] Ge, H. & Qian, H. Physical origins of entropy production, free energy dissipation, and their mathematical representations. *Phys Rev E* **81**, 051133 (2010).

[6] Phong, C., Markson, J. S., Wilhoite, C. M. & Rust, M. J. Robust and tunable circadian rhythms from differentially sensitive catalytic domains. *Proc Natl Acad Sci U S A* **110**, 1124–1129 (2013).

[7] Rust, M. J., Golden, S. S. & O'Shea, E. K. Light-driven changes in energy metabolism directly entrain the cyanobacterial circadian oscillator. *Science* **331**, 220–3 (2011).

[8] Van Kampen, N. G. *Stochastic processes in physics and chemistry* (Elsevier, Amsterdam, 1992).

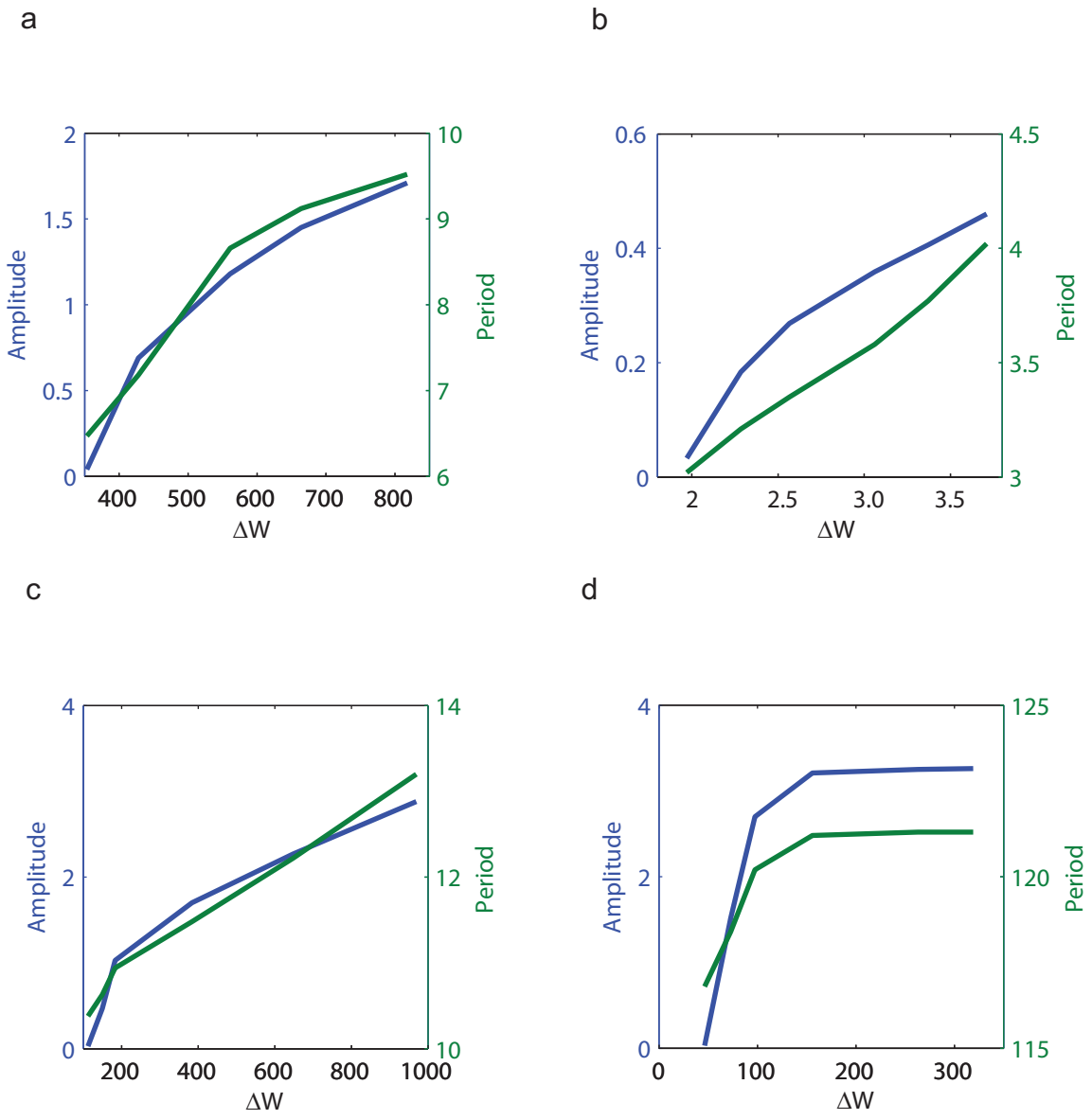

FIG. S1. The dependence of amplitude (A) and period (T) on energy dissipation for the four models: (a) activator-inhibitor, (b)repressilator, (c)brusselator, (d)glycolysis. For all the four cases, the critical free energy dissipation per period W_c is finite at the onset of the oscillation, i.e., $A = 0$.

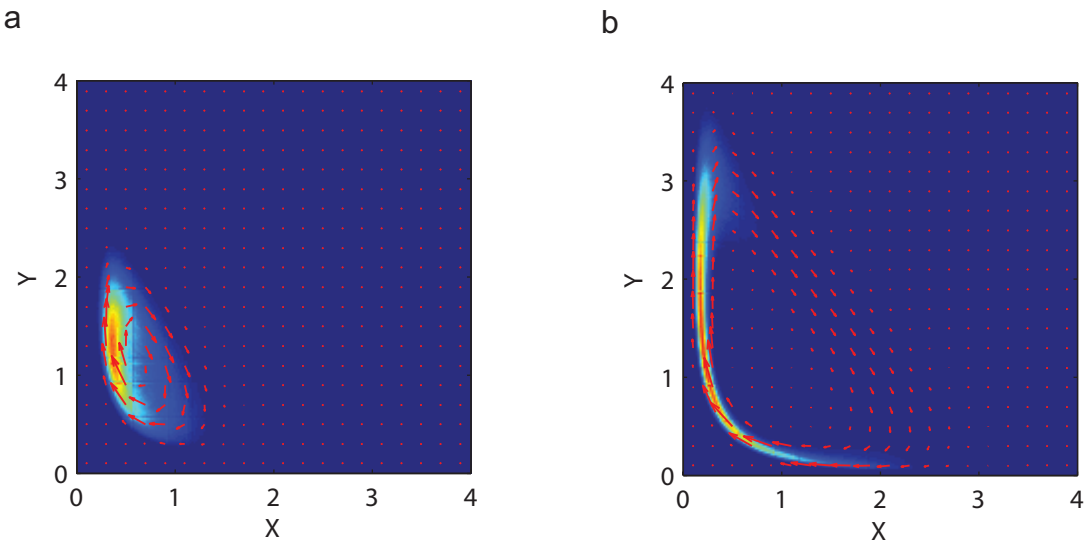

FIG. S2. Probability distributions and fluxes (red arrows) in the brusselator model. (a)$a = 0.18$, near the onset (bifurcation point), (b) $a = 0.12$, far from the bifurcation point. Results for other models are similar (not shown here), but have more dimensions.

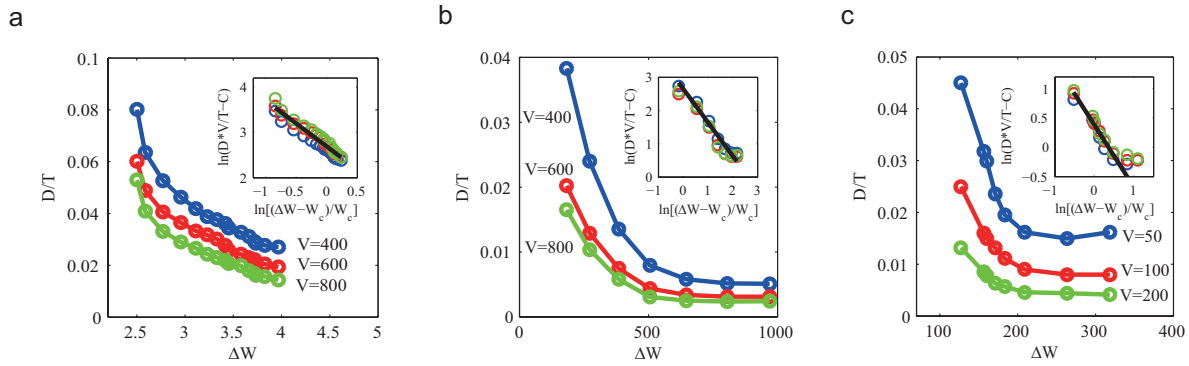

FIG. S3. Relation between the dimensionless diffusion constant (D/T) and free energy dissipation repressilator, brusselator and glycolysis. The insets are fitting results with equation $V \times D/T = C + W_0 \times (W - W_c)^{\alpha}$. (a) Repressilator, with fitting parameters $W_c = 1.75, W_0 = 25.9 \pm 3.21, \alpha = -1.098 \pm 0.078, C = 0.4 \pm 0.2$. (b) Brusselator, with fitting parameters $W_c = 100.4, W_0 = 846.3 \pm 158.2, \alpha = -1.006 \pm 0.031, C = 0.5 \pm 0.1$. (c) Glycolysis, with fitting parameters $W_c = 80.5, W_0 = 151.4 \pm 19.4, \alpha = -1.058 \pm 0.026, C = 0.5 \pm 0.3$.

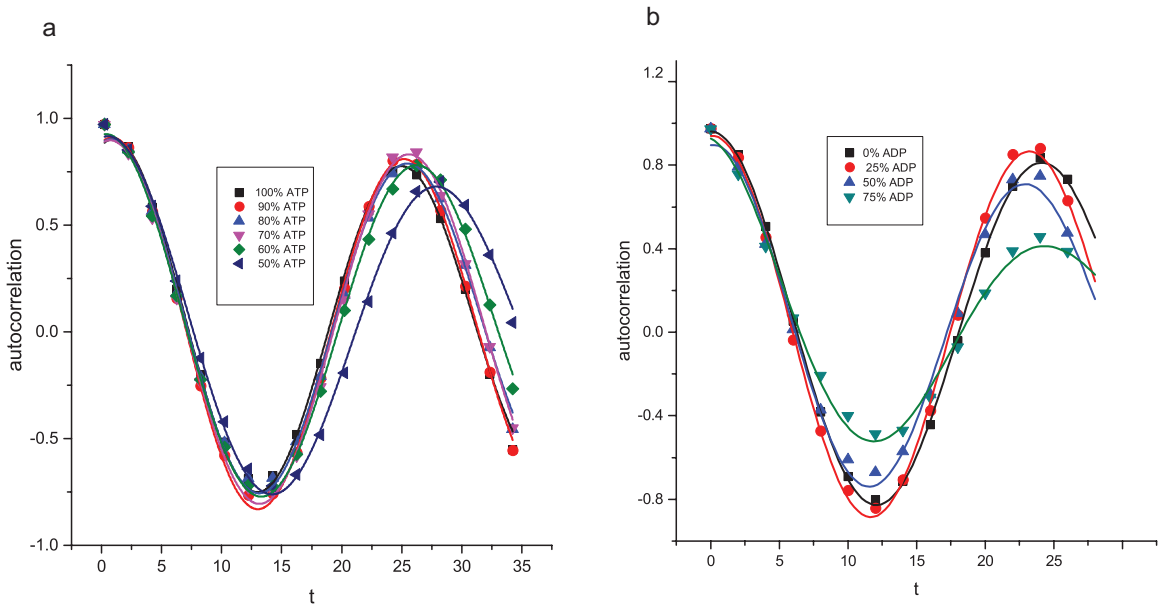

FIG. S4. Autocorrelation of experimental data from the reconstituted circadian clock system of the cyanobacteria system (the Kai system). The autocorrelation function of the phosphorylated KaiC were calculated from the original data and fitted by $A\cos(2\pi t/T)e^{-t/\tau}$. From the fits, we obtain he period T and the correlation tim τ, which are used in Fig. 4 in the main text. (a) Data (symbols) from Ref[7] with different ATP percentages. The lines are the fits. (b) Data from Ref[6] with different ADP percentages. The lines are the fits.

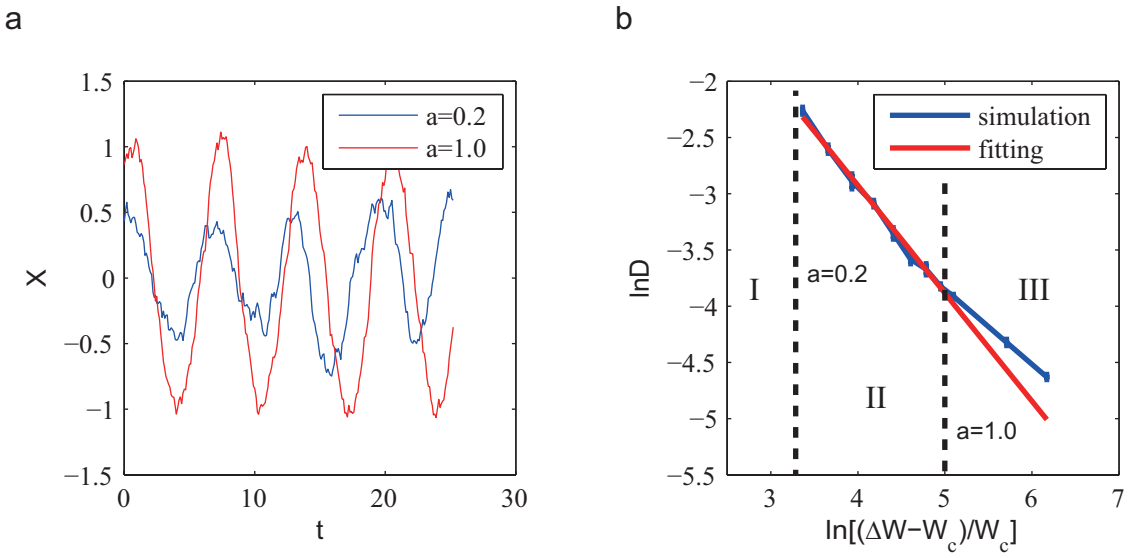

FIG. S5. The inverse relation between energy dissipation and phase diffusion are valid in limited regions. The simulation parameters for SL equation are $b = 1, c = 1, d = 1, \Delta = 0.02$. (a) Trajectories at the lower bound $a = \sqrt{2c\Delta} = 0.2$, and upper boundary $a = bc/d = 1.0$. (b) The inverse relation are valid in limited regions. Region I has phase ambiguity. Region II is the inverse relation region. Region III has the relation dominated by $(\Delta W - W_c)^{-1/2}$. The blue line is the simulation result, and the red line is the fitting with equation $D = W_0 \times (\Delta W - W_c)^{\alpha}$, with $W_c = 8\pi d/c = 25.1$, and $\alpha = -0.9784 \pm 0.0185, W_0 = 3.09 \pm 0.48$.

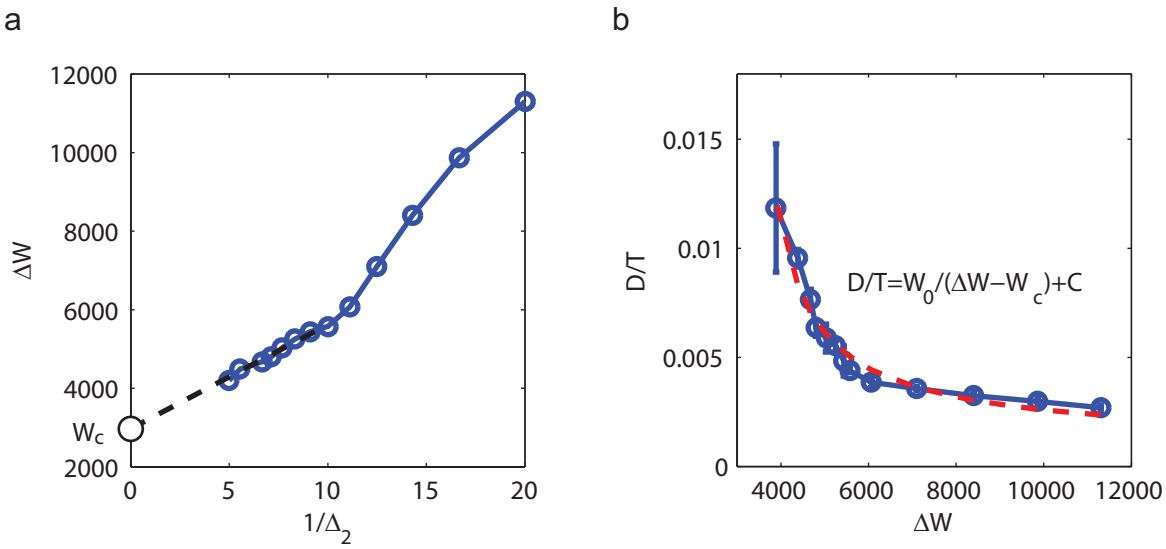

FIG. S6. Numerical simulation results of of the general Stuart-Landau equation (Eq. S24) with $a = 1, c = 1, b = 2, d = 1, \Delta_1 = 0.1$. We varied $\Delta_2 \in [0.05, 0.2]$. (a) Relationship between energy dissipation ΔW and noise strength Δ_2. When Δ_2 is large, ΔW decreases linearly with $1/\Delta_2$. The dashed line shows when $\Delta_2 \to \infty$, $\Delta W \to W_c \approx 2967$ (black circle). (b) The peak time diffusion constant D/T versus ΔW. The red dashed curve is the fitting inverse proportional relation, with parameters $W_0 = 10.2, W_c = 2967, C = 0.0011$.

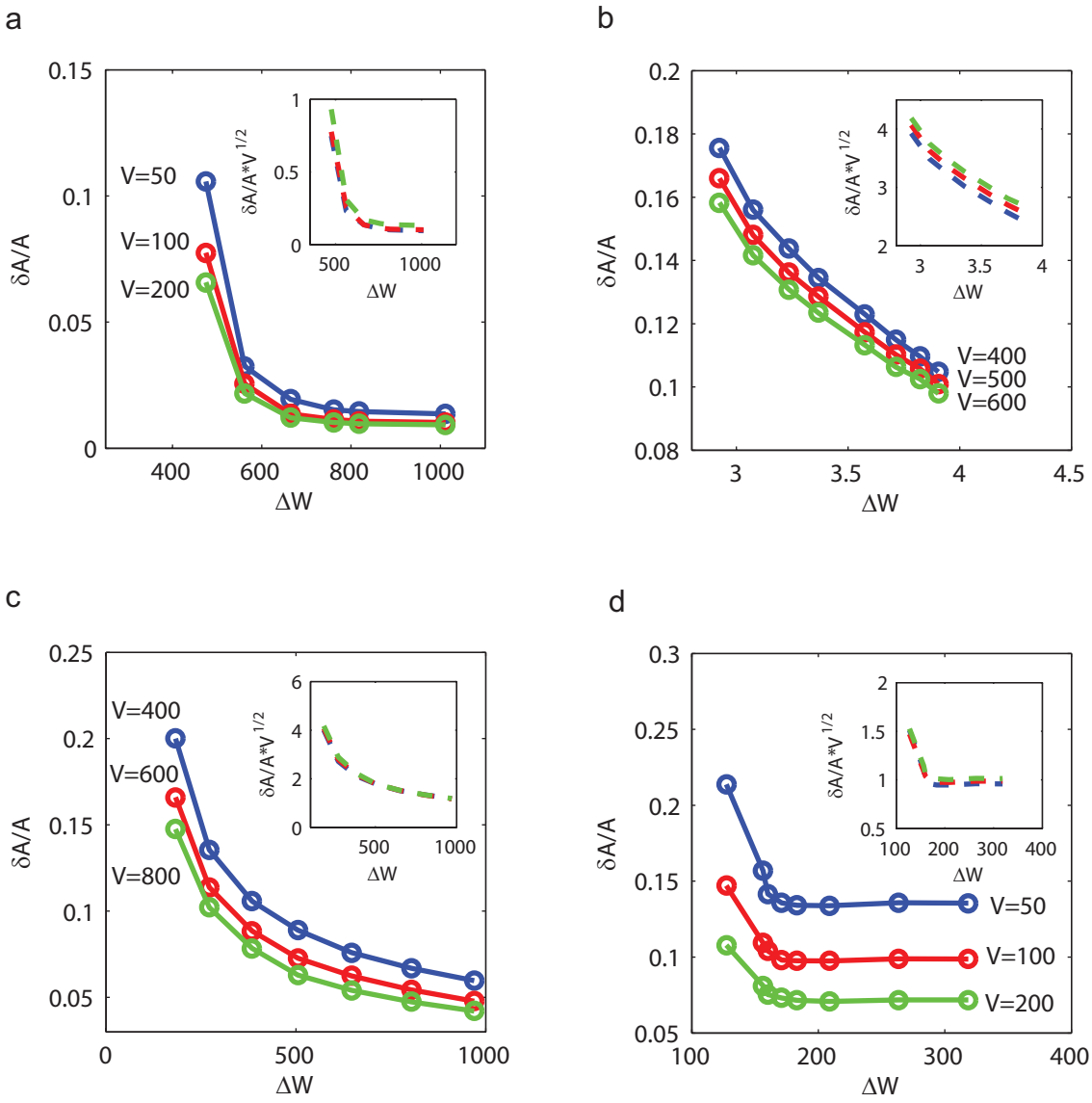

FIG. S7. Relation between relative amplitude fluctuation $\delta A/A$ and free energy dissipation ΔW for the four models. (a) activator-inhibitor; (b)repressilator; (c)brusselator; (d)glycolysis. Data for different volumes collapses (insets) when we scaled amplitude fluctuation with $1/\sqrt{V}$.

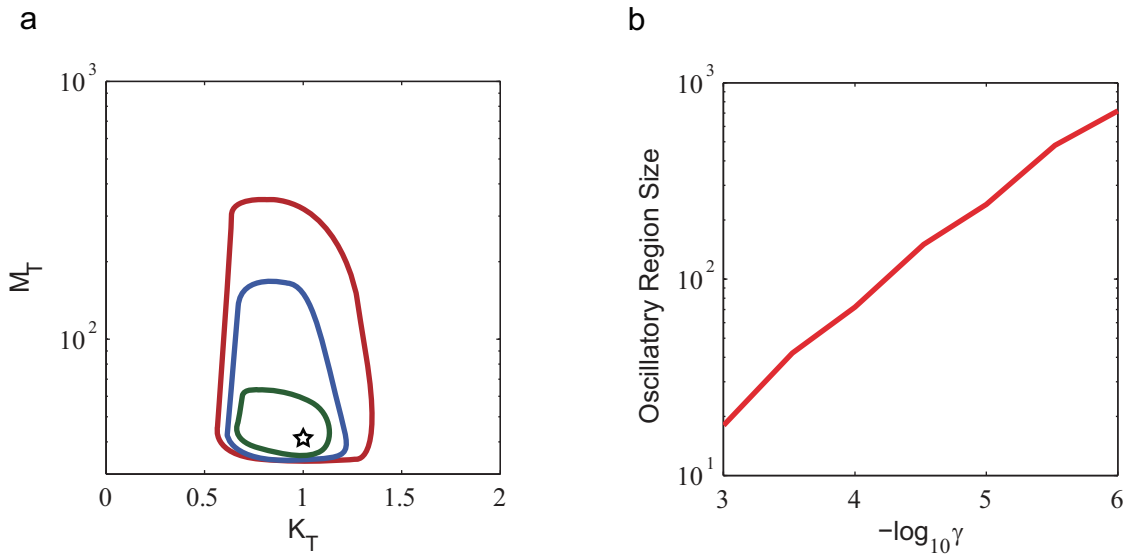

FIG. S8. The relationship between functional robustness and free energy dissipation. (a) The green, blue and red curves in the (M_T, K_T) space correspond to the boundaries inside which oscillations exist for $\gamma = 10^{-3}$, $\gamma = 10^{-4}$ and $\gamma = 10^{-5}$, respectively. The star indicates the parameters in main text Fig1 a. (b) Robustness, defined as the area of oscillation in the parameter space, increases as γ decreases. This means that higher free energy consumptions (on average) is needed for higher robustness against parameter variations in achieving oscillatory behaviors.